Supporting information

Fig. S1-S5. IR spectra of the complexes (**1-4a**).

Fig. S6. Electronic spectra of the complexes (**1-4a**).

Fig. S7-11. ^{1}H-NMR spectra of the complexes (**1-4a**).

Fig. S12. ORTEP diagram of complex **2** with hydrogen bonding.

Fig. S13. ORTEP diagram of complex **4** with hydrogen bonding.

Fig. S14. ESI-MS spectrum of the complex **1**.

Fig. S15. ESI-MS spectrum of the complex **3**.

Fig. S16. Synchronous spectra of BSA (1×10^{-6} M) in the absence and presence of complexes **1-4** (0-70 μM) in the wavelength difference of $\Delta\lambda = 60$ nm.

Fig. S17 MCF-7 cells were treated with different concentrations of compounds (3.125, 6.25, 12.5, 25, 50, 100 μM) for 24 h. Cell viability was assessed by cell proliferation (MTT) assay. Error bars represent the standard deviation of the mean (n=3).

Table S1. Hydrogen bonds for complexes **2** and **4** [A˚ and °].

DNA binding studies

The experiments involving CT-DNA were performed in double distilled water with tris(hydroxymethyl)aminomethane (Tris, 5 mM) and sodium chloride (50 mM) and adjusted to pH 7.2 with hydrochloric acid. The concentration of CT-DNA was determined by UV absorbance at 260 nm. The molar absorption coefficient, ε_{max} 260, was taken as 6600 M^{-1} cm^{-1}.[6] CT-DNA solution of various concentrations (0-50 μM) dissolved in Tris-HCl (pH 7.2) were added to the palladium complexes **1-4** (10 μM dissolved in a DMSO-H_2O mixture). Absorption spectra were recorded after equilibrium at 20 ºC for 10 min. The intrinsic binding constant K_b was determined by using the Stern-Volmer equation (1).[1]

$$([DNA] / [\varepsilon_a - \varepsilon_f]) = [DNA] / [\varepsilon_b - \varepsilon_f] + 1/ K_b[\varepsilon_b - \varepsilon_f] \qquad (1)$$

The absorption coefficients ε_a, ε_f, and ε_b correspond to A_{obsd}/[DNA], the extinction coefficient for the free complexes and the extinction coefficient for the complexes in the fully bound form, respectively. The intrinsic binding constant K_b can be obtained from the ratio of the slope to the intercept in plots of [DNA]/ [ε_a - ε_f] versus [DNA].

Competitive binding with ethidium bromide

To find out the exact mode of attachment of CT-DNA to the complexes, fluorescence quenching experiments of EB-DNA were carried out by adding 10 μL portion of 10 μM palladium(II) complexes every time to the sample containing 10 μM EB, 10 μM DNA and Tris buffer (pH 7.2). Before the measurements, the system was shaken and incubated at room temperature for ~5 min. The emission spectra were recorded at 530-750 nm. On the basis of the classical Stern-Volmer equation, the quenching constant has been analysed (2).

$$I_0/I = K_{sv}[Q] + 1 \qquad (2)$$

Where I_0 and I represent the emission intensities in the absence and presence of the complexes, respectively, K_{sv} is the quenching constant, and [Q] is the concentration ratio of the complex. The K_{sv} values have been obtained as a slope from the plot of I_o/I versus [Q].

Further, the apparent DNA binding constant (K_{app}) were calculated using the following equation,

$$K_{EB}\,[EB] = K_{app}[complex]$$

(Where [complex] is the value at a 50 % reduction in the fluorescence intensity of EB, K_{EB} ($1.0 \times 10^7\ M^{-1}$) is the DNA binding constant of EB, [EB] is the concentration of EB =10 μM).

DNA cleavage studies

The cleavage of DNA was monitored by using agarose gel electrophoresis. Supercoiled pBR322 DNA (100 mg) in 5 % DMSO and 95 % Tris buffer (5 mM, pH 7.2) with 50 Mm NaCl was incubated at 37 °C in the absence and presence of compounds. The DNA, compound and sufficient buffer were premixed in a vial, and the reaction was allowed to proceed for 2 h at 37 °C. The samples were then analyzed by 1.5 % agarose gel electrophoresis in tris-acetic acid-ethylenediaminetetraacetic acid buffer. The gel was stained with 0.5 μg cm^{-3}ethidium bromide before migration. After electrophoresis at 50 V for 3 h, the gel was illuminated and the digital images were analyzed by gel documentation system (SYNGEN USA).[2]

Bovine serum albumin binding study

BSA solution (10 μM) was prepared in phosphate buffer of pH 7.2 and stored in the dark at 4 °C for use. The excitation wavelength of BSA at 280 nm and the emission at 346 nm were monitored for the protein binding studies. The excitation and emission slit widths and scan rates were maintained constant for all of the experiments. Concentrated stock solution of complexes were prepared by dissolving the compounds in DMSO and diluted suitably with deionised water to required concentrations for all the experiments (1 % DMSO in the final solution). Quenching of the emission intensity of tryptophan residues of BSA at 346 nm (excitation wavelength at 276 nm) was monitored using compound as quenchers with increasing compound concentration. The possible quenching mechanism has been interpreted using the Stern-Volmer equation (2).

When small molecule bind to the active site of BSA, the equilibrium binding constant and the number of binding sites can be analysed by using the Scatchard equation (4).

$$\log [F_0 - F/F] = \log K + n \log[Q] \qquad (4)$$

Where K is the binding constant of quencher with BSA, n is the number of binding sites, F_0 and F are the fluorescence intensity in the absence and the presence of the quencher. Which can be determined by the slope and the intercept of the double logarithm regression curve of log $[(I_0-I)/I]$ versus log [Q]. Synchronous fluorescence spectra of BSA with various concentrations of complexes (0-100 μM) were obtained from 300 to 500 nm when Δλ= 60 nm and from 290 to 500 nm when Δλ

= 15 nm. The excitation and emission slit widths were 5 and 6 nm, respectively. Fluorescence and synchronous measurements were performed by using a 1 cm quartz cell on a JASCO FP 6600 spectrofluorometer.

Three dimension fluorescence spectra measurement

The 3D fluorescence spectra of BSA were recorded with and without complexes. Protein solution at 10 μM was transferred to a quartz cell, diluted with 2.0 mL phosphate buffer and mixed well. To this, 10 μM of complexes was added and the 3D fluorescence spectra were recorded by scanning excitation wavelength in the range of 200–350 nm and emission wavelength from 220 to 500 nm at an interval of 10 nm. The scanning parameters were the same as in the fluorescence quenching experiments.

Cytotoxicity studies

3-(4,5-Dimethylthiazol-2-yl)-2,5-diphenyltetrazolium bromide (MTT) assay[3]

MTT, upon reduction by NAD(P)H-dependent cellular oxidoreductase enzymes present in the cytoplasm of metabolically active cells, forms formazan as a purple insoluble product. The amount of formazan estimated by a spectral method correlates with the number of live cells and provides a quantitative measurement of the cytotoxicity of the compound. The IC_{50} values were obtained from nonlinear regression using GraphPad Prism 5.[4] About 6000 cells of MCF-7 (human breast cancer cells) were taken in each well of a 96-well culture plate and incubated for 24 hours in a CO_2 incubator. After incubation, different concentrations (3.12, 6.25, 12.5, 25, 50, 100 μM) of the compounds dissolved in DMSO were added to the cells. After appropriate incubation time (24 h for complexes, metal precursors, ligands and 1,3-bis (diphenylphosphino)propane), the wells were treated with 20 μl MTT (5 mg/ml phosphate-buffered saline, PBS) and incubated for 3 h. The purple formazan crystals obtained were dissolved in 200μl DMSO and the absorbance was measured at 570 nm in Molecular Devices Spectra Max M5 plate reader. Data were obtained as the average of three independent sets of experiments, all performed in triplicate for each concentration.[3]

Morphological Changes of MCF7 cells using phase contrast inverted microscope

Observation of morphological changes of apoptotic cells was performed according to the method with slight modifications.[5] Briefly, MCF-7 cells were seeded into 24-well plate and incubated overnight to attach. Then, the cells were treated with or without test compounds (control) at different concentrations of 6.25 and 12.5 μM for complexes **1-4** was incubated 24 h at 37 °C with

5 % CO_2. The morphological changes of the cells were observed using an inverted light microscope at 100 X magnification.

Acridine orange/ethidium bromide staining assay

Acridine orange/ethidium bromide staining was carried out by the method of Gohel *et al*.[6] and MCF-7 cells were plated in a 24-well plates. They were allowed to grow at 37 °C in a humidified CO2 incubator. Then the cells were treated with IC_{50} concentrations of complexes **2** and **3** for 24 h. The culture medium was aspirated from each well and the cells were gently rinsed twice with PBS at room temperature. Then equal volumes of cells from control and metal complexes treated were mixed with 100 ml of dye mixture (1:1) of acridine orange and ethidium bromide and viewed immediately by fluorescence microscopy.

References

1. (a) A. Wolfe, G. H. Shimer and T. Meehan, *Biochemistry,* 1987, **26**, 6392-6396. (b) G. Cohen, H. Eisenberg, *Biopolymers,* 1969, **8**, 45-55.
2. S. Sathiyaraj, K. Sampath, R. J. Butcher, R. Pallepogu and C. Jayabalakrishnan, *Eur. J. Med. Chem.*, 2013, **64**, 81-89.
3. T. Mossman, *J. Immunol. Methods*, 1983, **65**, 55-63.
4. H. J. Motulsky, Prism 5 Statistics Guide, GraphPad Software Inc., San Diego, CA 2007 http://www.graphpad.com.
5. P. Moongkarndi, N. Kosem, S. Kaslungka, O. Luanratana, N. Pongpan and N. Neungton, *J. Ethnopharmacol*., 2004, **90**, 161-166.
6. A. Gohel, M. B. McCarthy and G. Gronowicz, *Endocrinology*, 1999, **140**, 5339-5347.

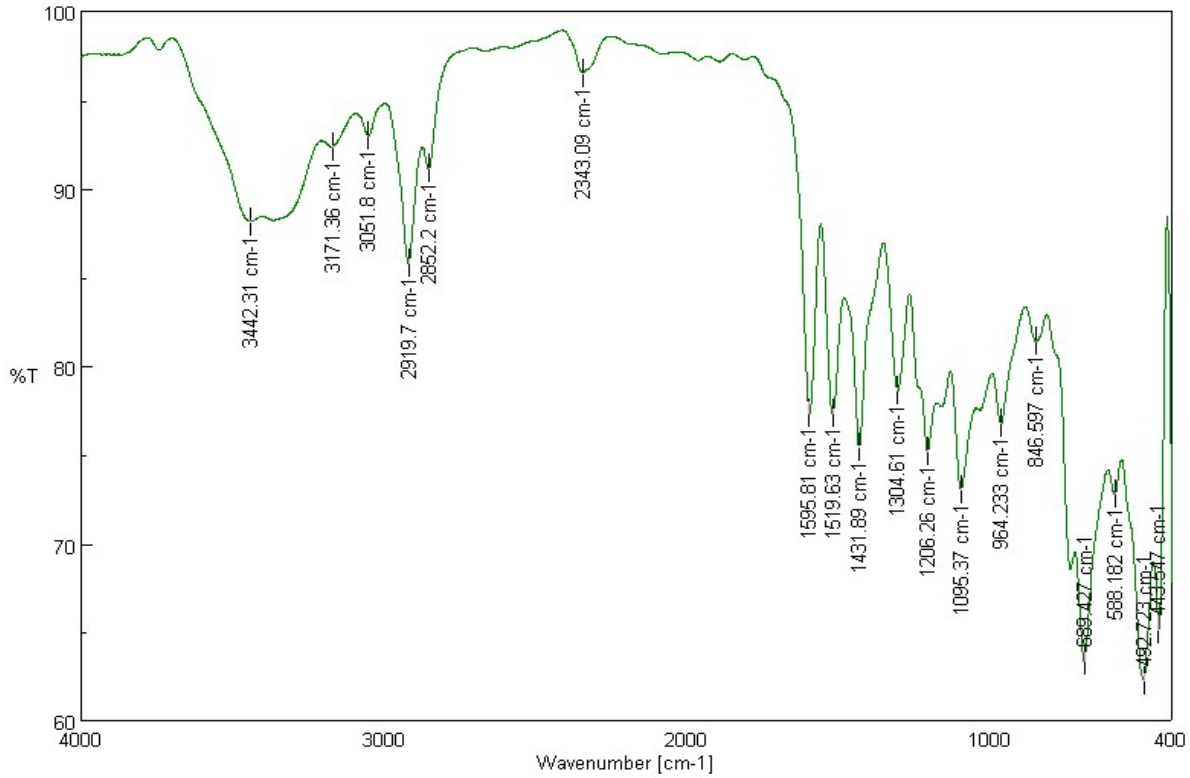

Fig. S1. IR spectrum of complex [Pd(H-Msal-tsc)(Msal-taz)].Cl **(1)**

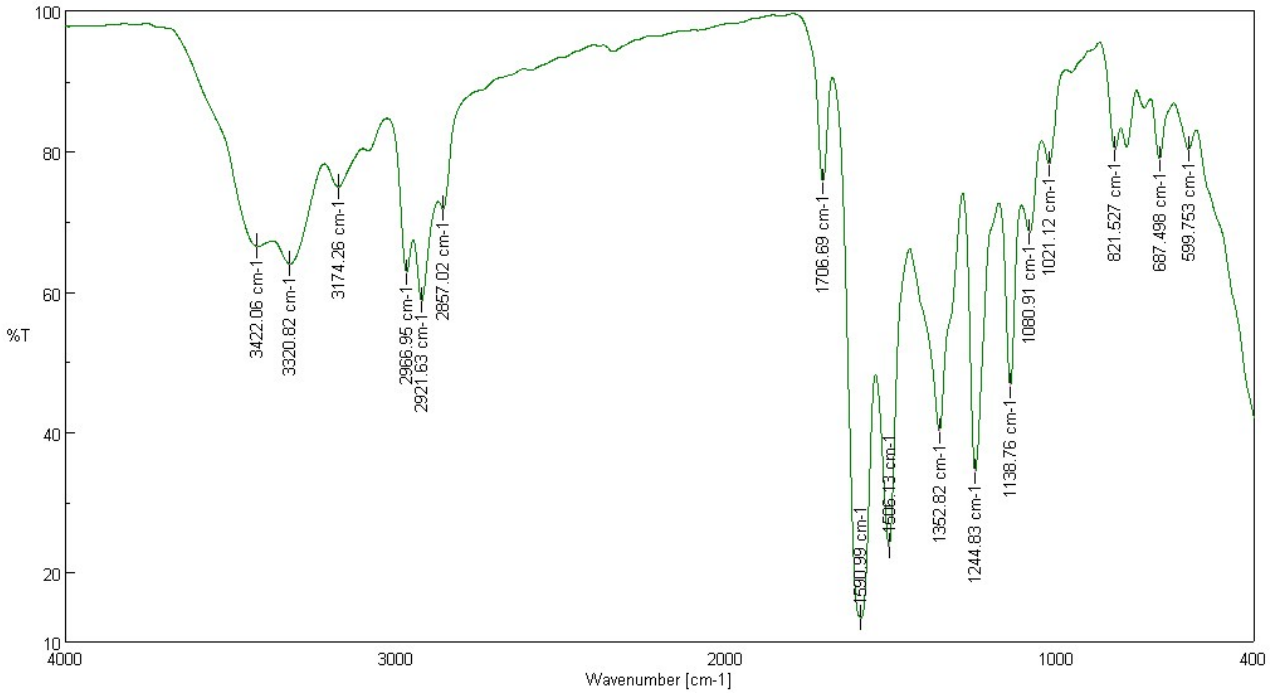

Fig. S2. IR spectrum of complex [Pd(H-Msal-mtsc)(Msal-mtaz)].Cl **(2)**

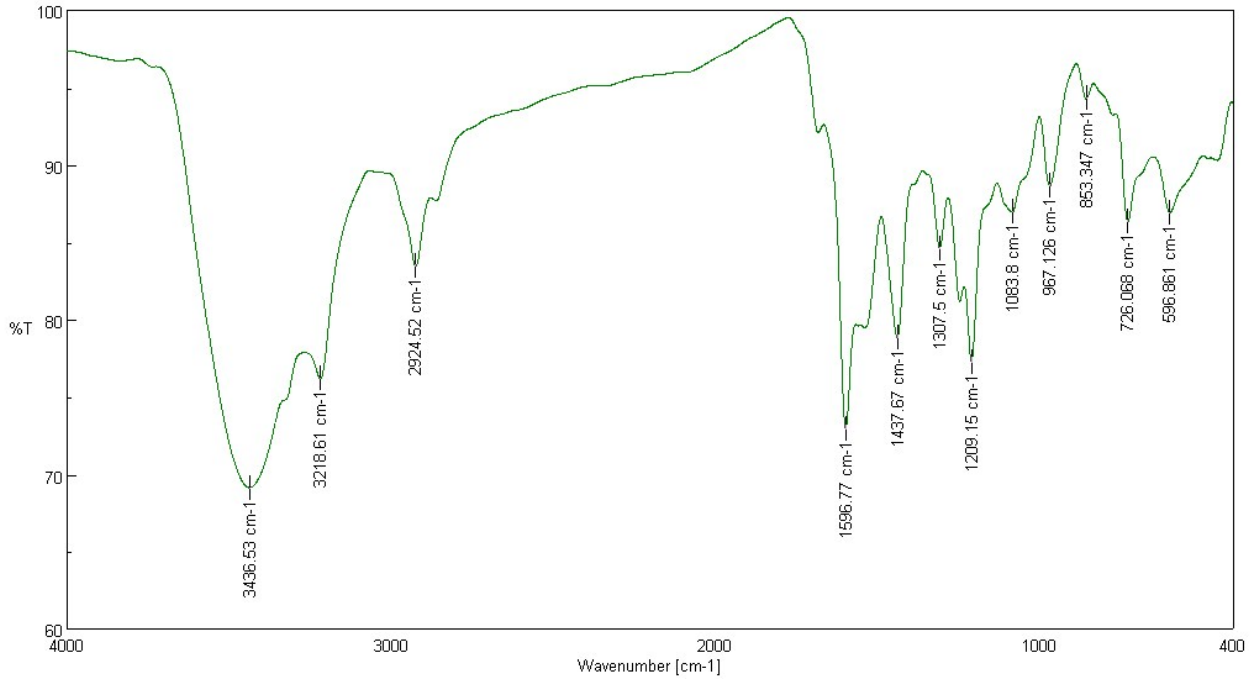

Fig. S3. IR spectrum of complex [Pd(H-Msal-etsc)(Msal-etaz)].Cl **(3)**

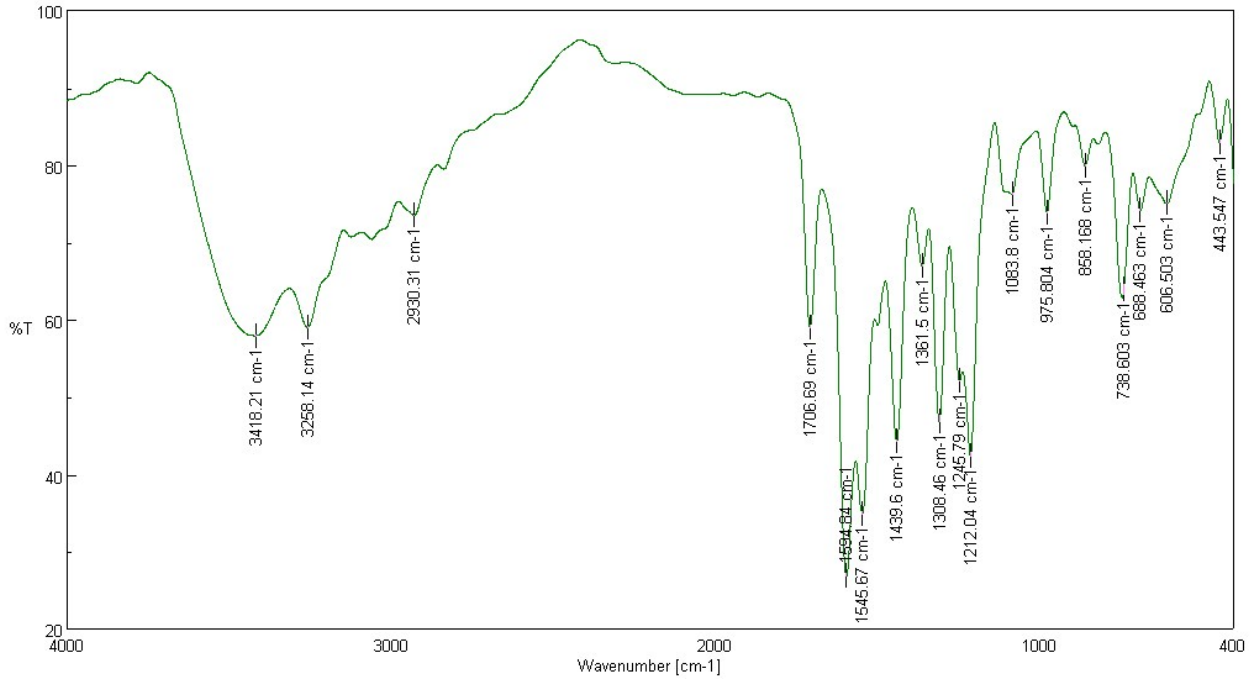

Fig. S4. IR spectrum of complex $[Pd_2((Msal\text{-}ptsc)(Msal\text{-}ptaz))_2].Cl$ **(4)**

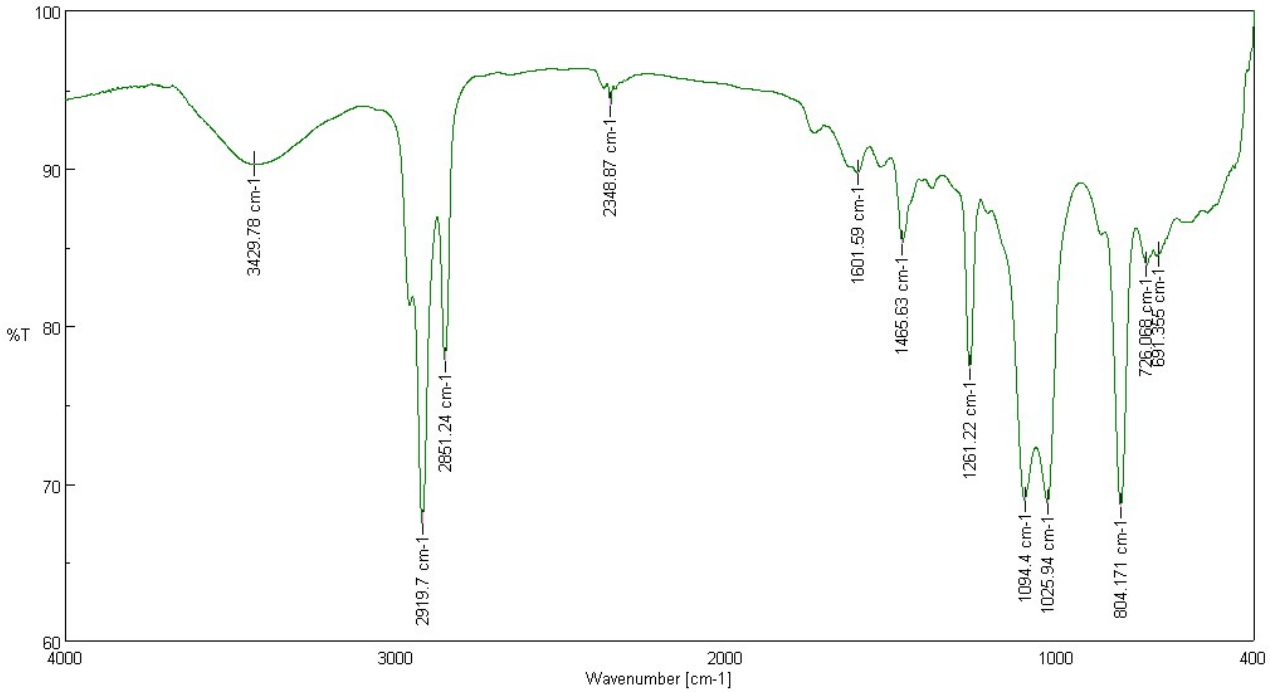

Fig. S5. IR spectrum of complex $[PdCl_2(dppp)]$**(1a-4a)**

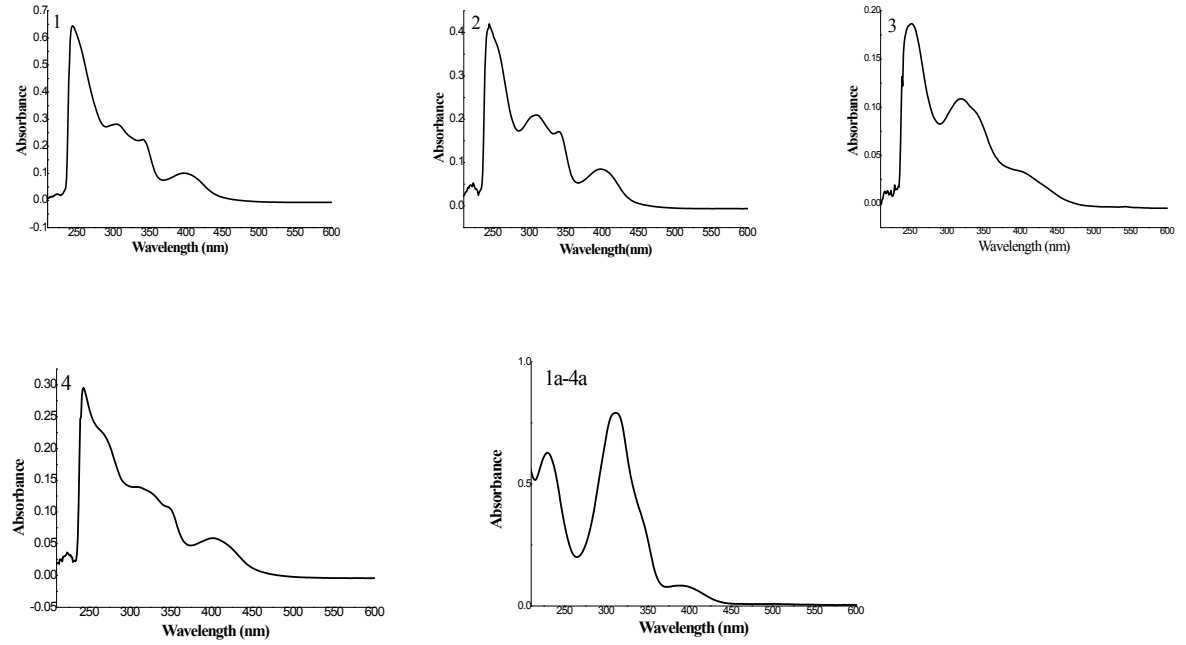

Fig. S6. Electronic spectra of complexes **1-4a**

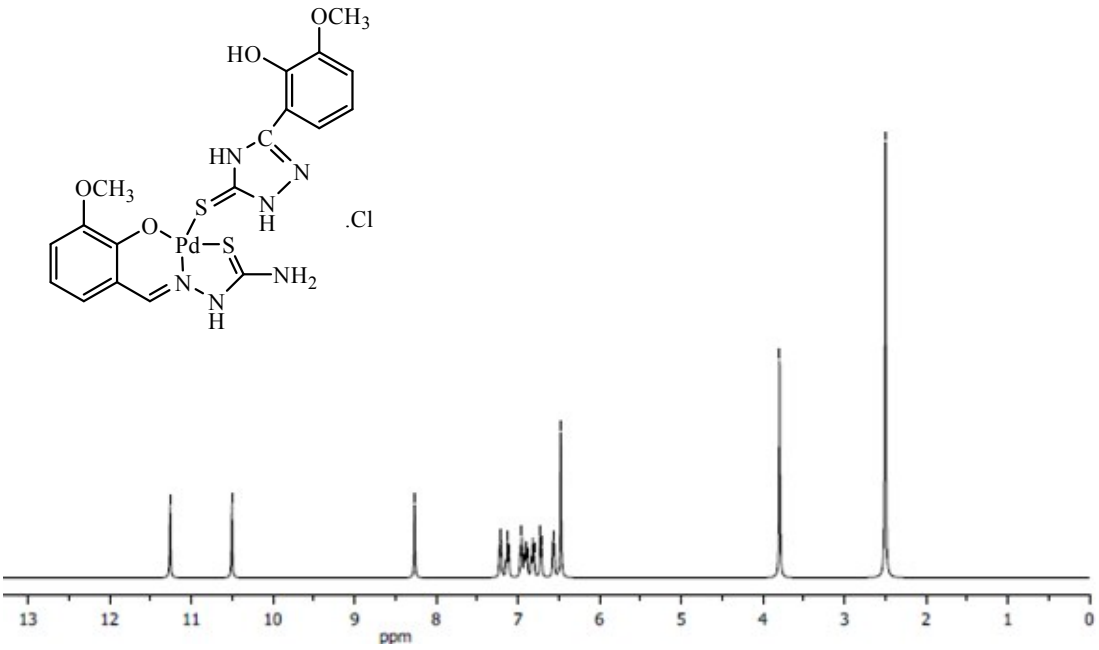

Fig. S7. [1]H-NMR spectrum of complex [Pd(H-Msal-tsc)(Msal-taz)].Cl **(1)**

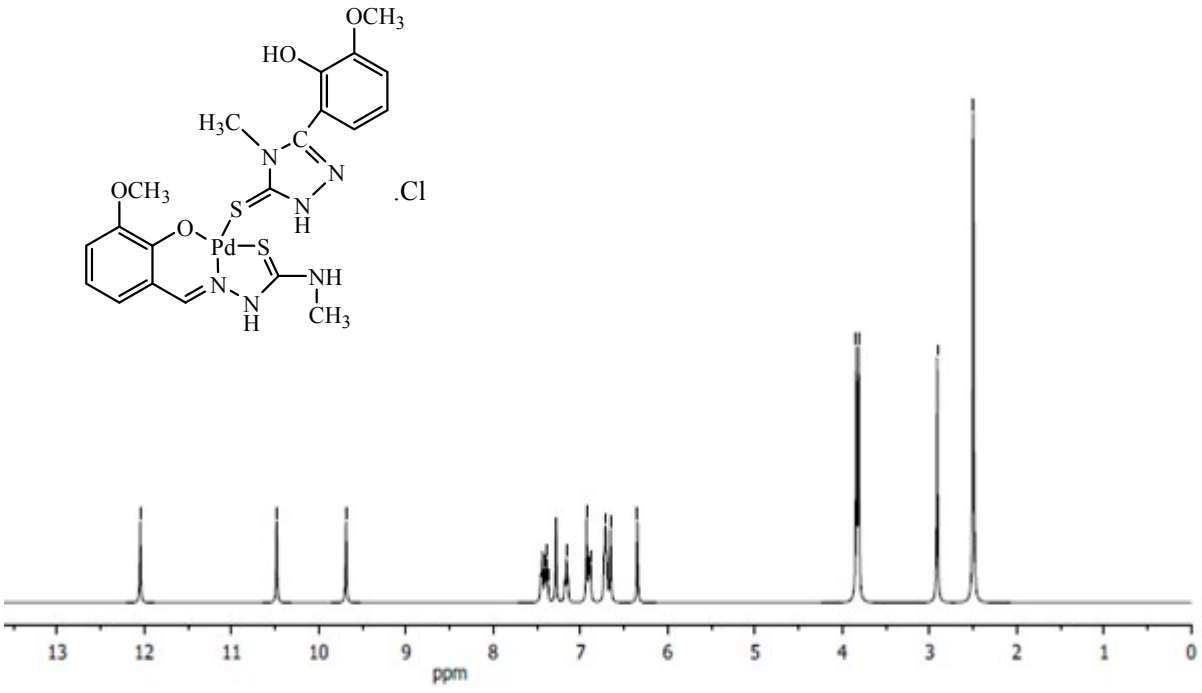

Fig. S8. [1]H-NMR spectrum of complex [Pd(H-Msal-mtsc)(Msal-mtaz)].Cl **(2)**

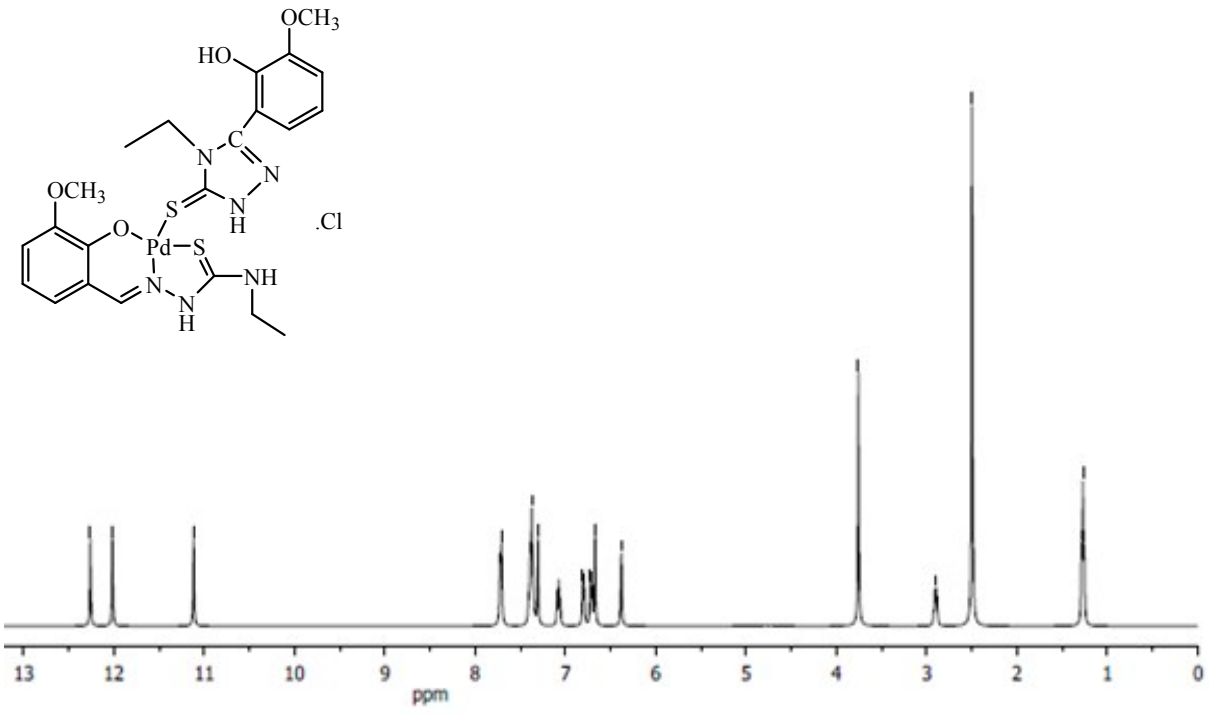

Fig. S9. ^{1}H-NMR spectrum of complex [Pd(H-Msal-etsc)(Msal-etaz)].Cl **(3)**

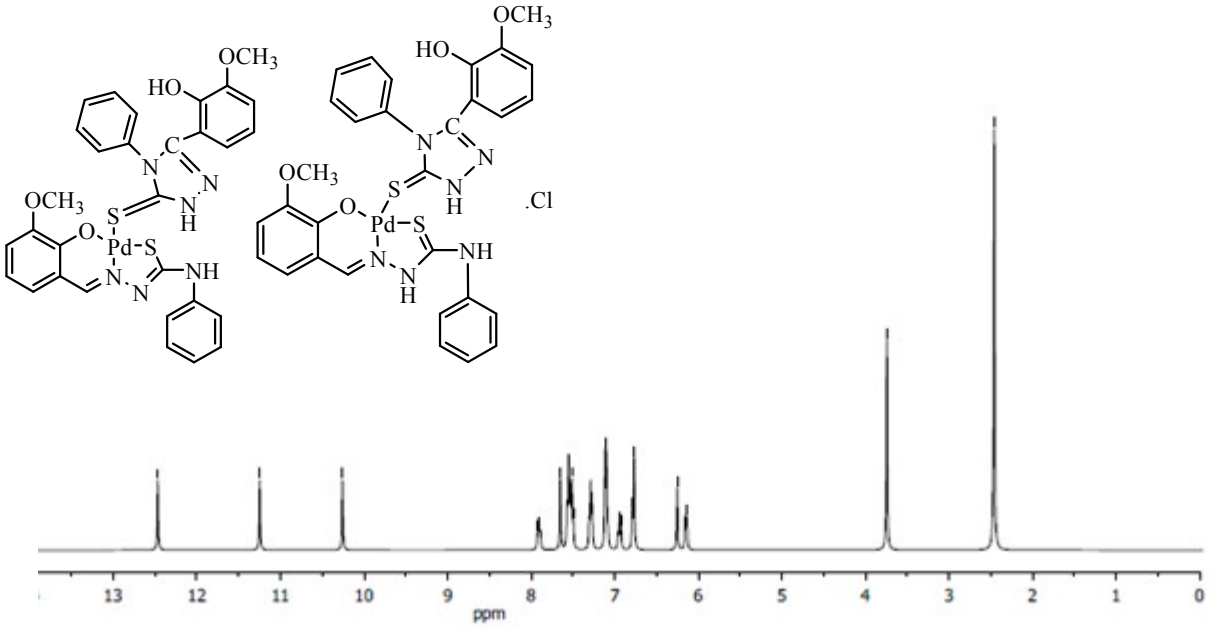

Fig. S10. ^{1}H-NMR spectrum of complex [Pd_2((Msal-ptsc)(Msal-ptaz))$_2$].Cl **(4)**

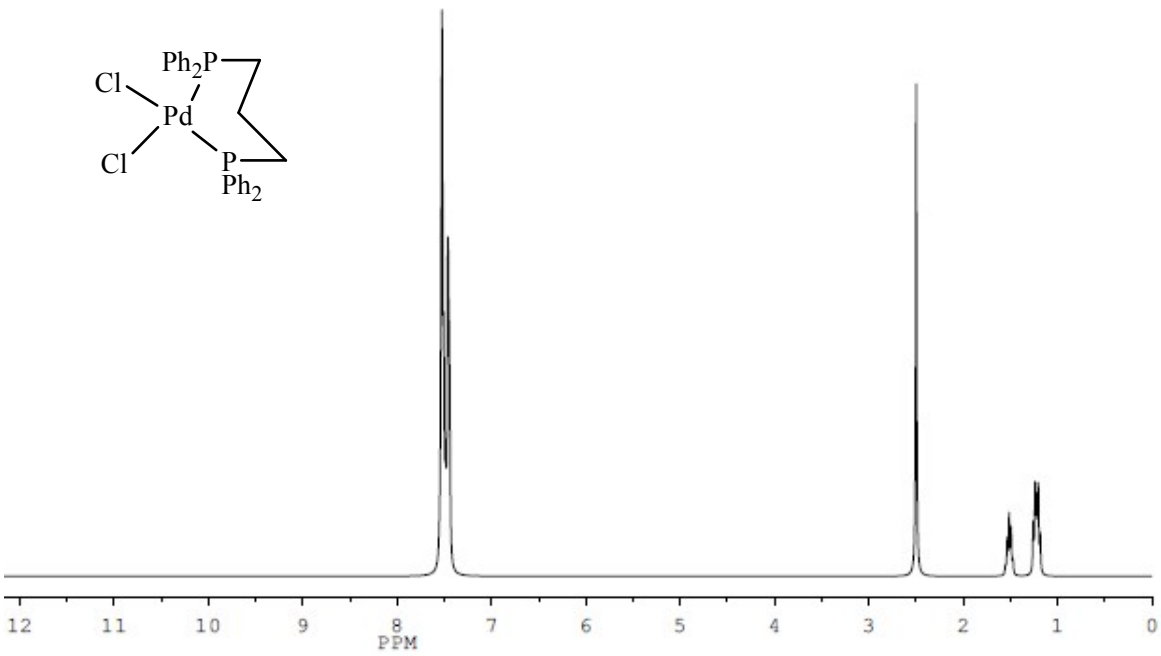

Fig. S11. ^{1}H-NMR spectrum of complex [$PdCl_2$(dppp)] **(1a-4a)**

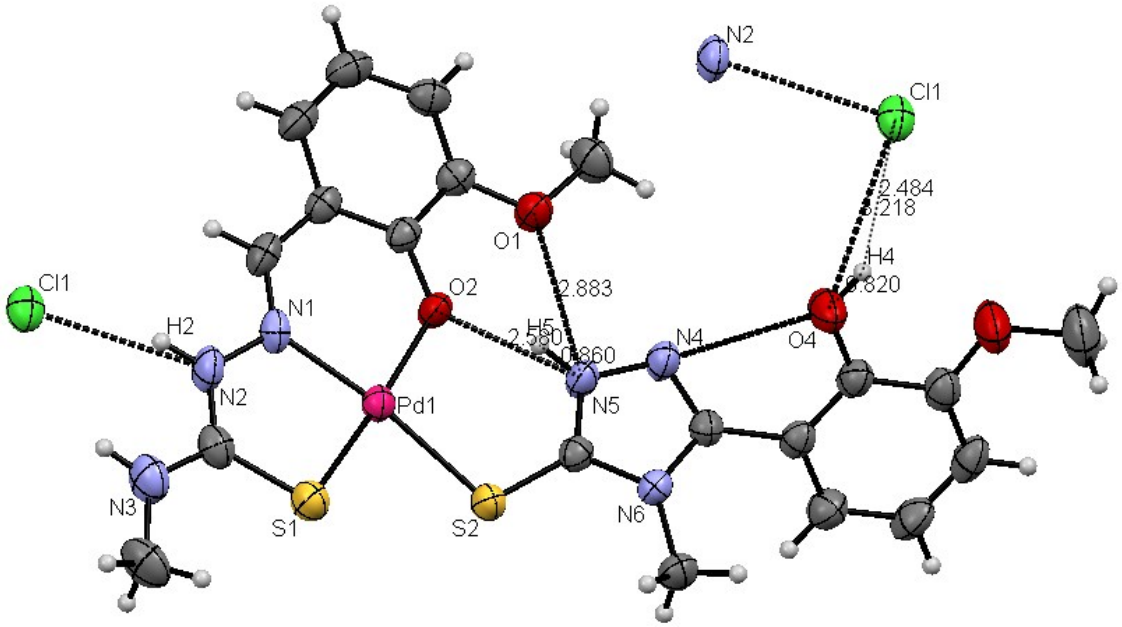

Fig. S12. ORTEP diagram of complex **2** with hydrogen bonding.

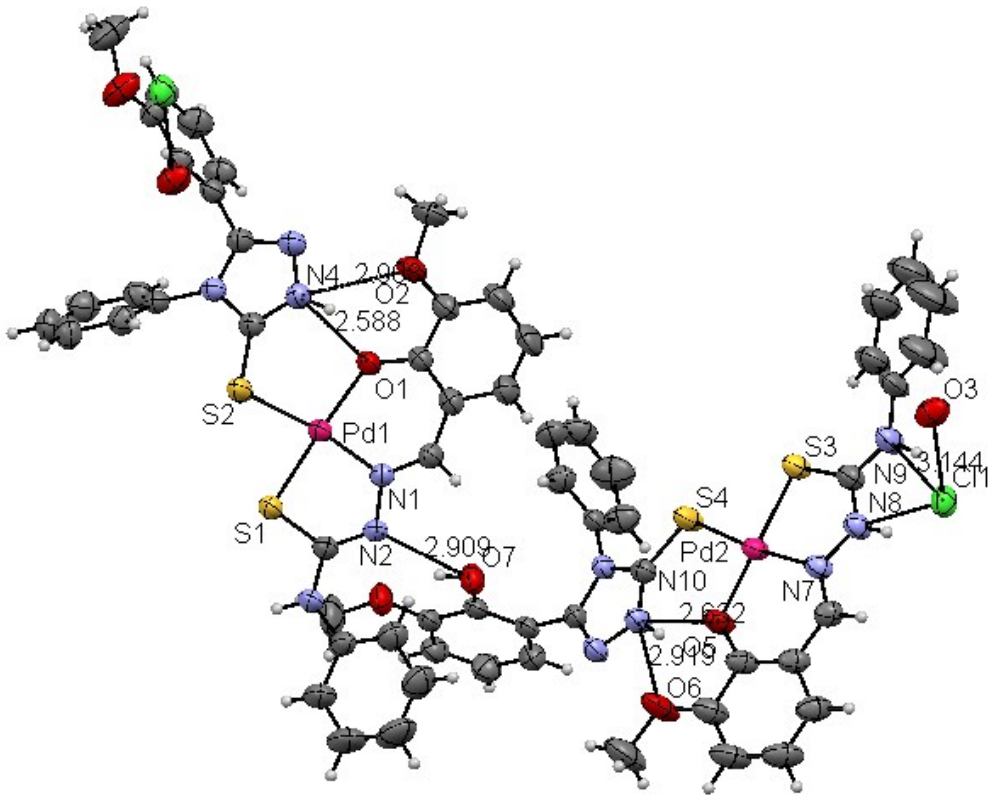

Fig. S13. ORTEP diagram of complex **4** with hydrogen bonding.

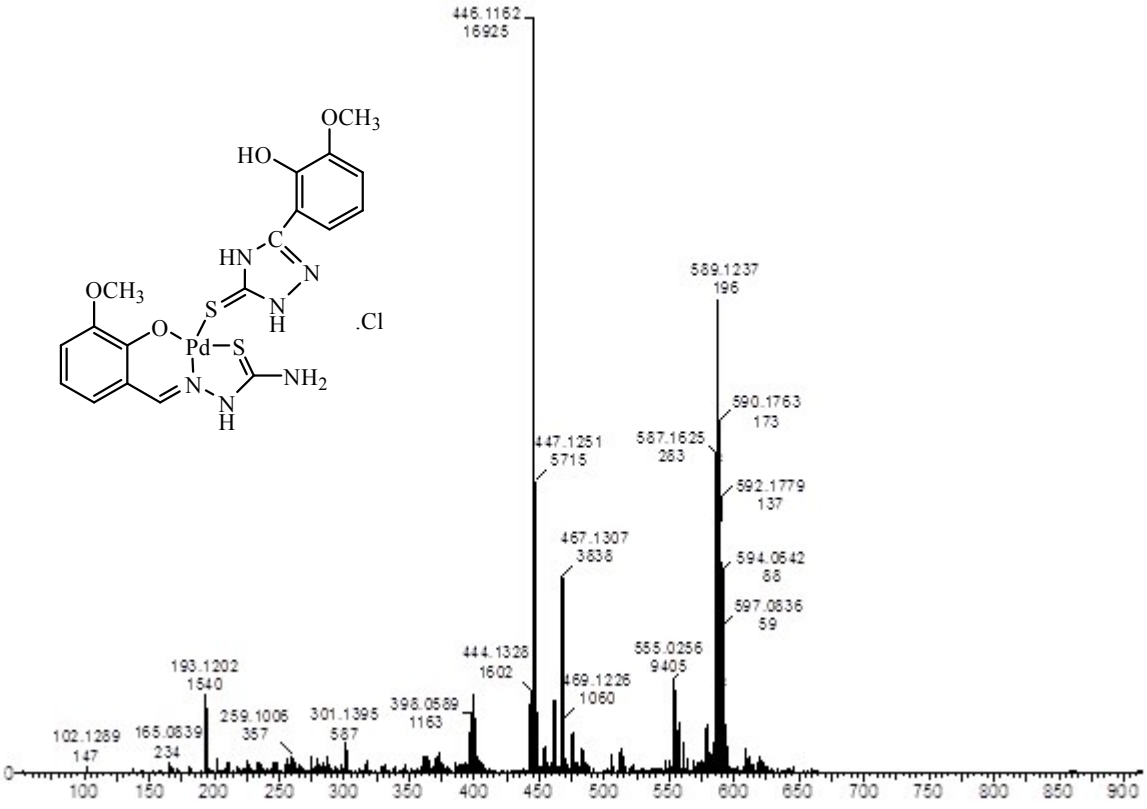

Fig. S14. ESI-MS spectrum of [Pd(H-Msal-tsc)(Msal-taz)].Cl **(1)**

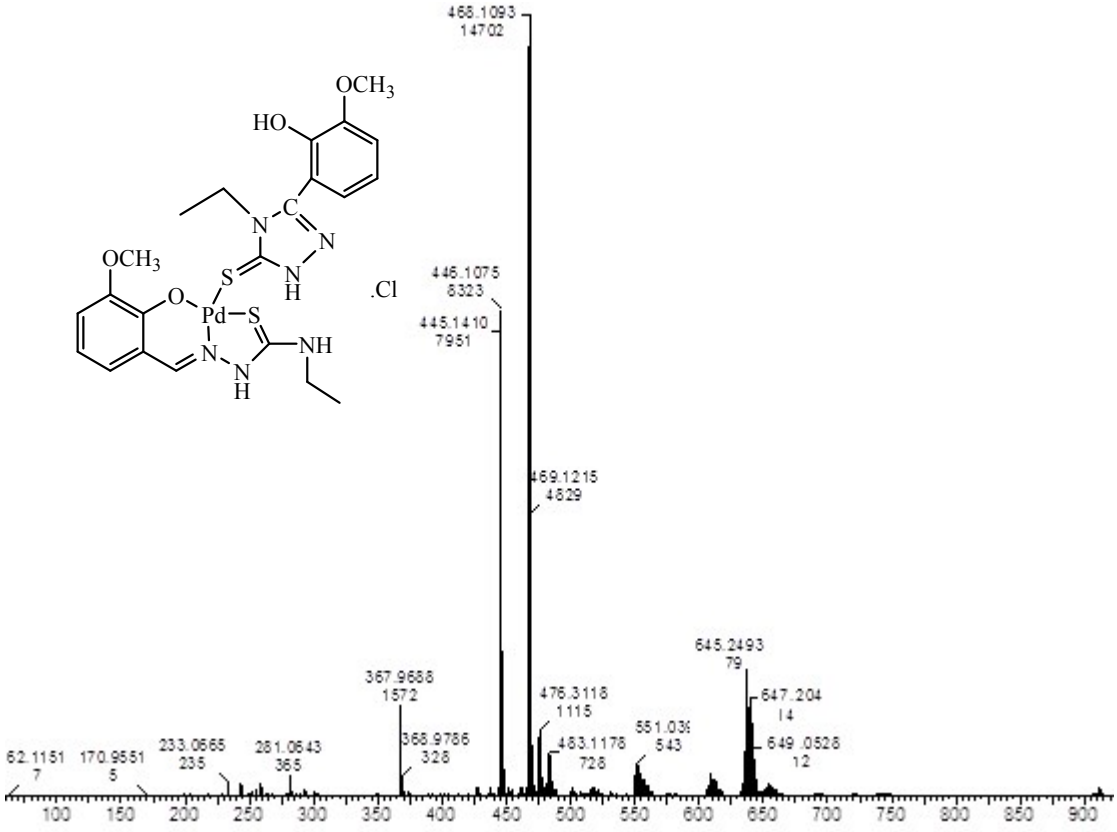

Fig. S15. ESI-MS spectrum of [Pd(H-Msal-etsc)(Msal-etaz)].Cl **(3)**

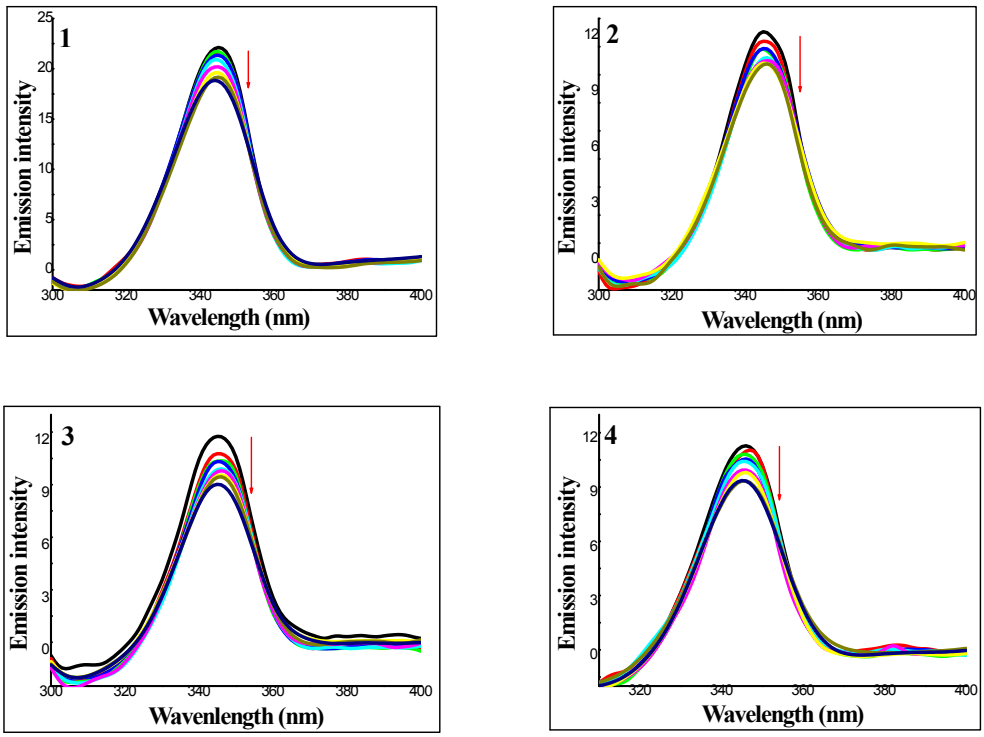

Fig. S16. Synchronous spectra of BSA (10 μM) in the absence and presence of complexes **1-4** (0-70 μM) in the wavelength difference of Δλ = 60 nm.

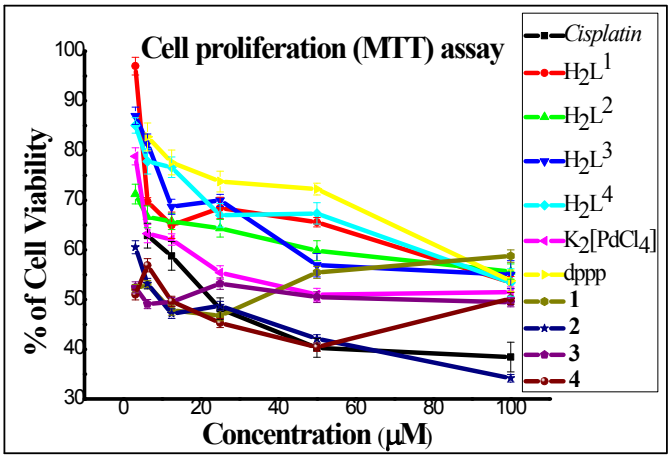

Fig. S17 MCF-7 cells were treated with different concentrations of compounds (3.125, 6.25, 12.5, 25, 50, 100 μM) for 24 h. Cell viability was assessed by cell proliferation (MTT) assay. Error bars represent the standard deviation of the mean (n=3).

Table S1. Hydrogen bonds for complexes **2** and **4** [A˚ and °]

D–H···A	d(D–H)	d(H···A)	d(D···A)	<(DHA)
[Pd(H-Msal-mtsc)(Msal-mtaz)].Cl **(2)**				
N(5)-H(5)...O(1)	0.860	2.245	2.883	130.97
N(5)-H(5)...O(2)	0.860	1.804	2.580	149.18
O(4)-H(4)...N(4)	0.820	3.630	2.966	139.70
O(4)-H(4)...Cl(1)	0.820	2.484	3.218	149.61
N(2)-H(2)...Cl(4)	0.859	2.290	3.043	163.55
Symmetry operation: (x, y, z); (-x, ½+y, ½-z); (-x,-y, -z); (x, ½-y, ½+z)				
$[Pd_2((Msal\text{-}mtsc)(Msal\text{-}mtaz))_2]$.Cl **(4)**				
N(4)-H(4)...O(1)	0.860	1.804	2.588	150.19
N(4)-H(4)...O(2)	0.860	2.259	2.908	132.31
N(10)-H(10)...O(5)	0.860	1.865	2.632	147.60
N(10)-H(10)...O(6)	0.860	2.232	2.919	136.79
O(7)-H(7)...N(2)	0.860	2.166	2.909	150.82
O(3)-H(3)...Cl(1)	0.820	2.407	3.204	164.28
N(8)-H(8)...Cl(1)	0.860	2.293	3.055	147.75
N(9)-H(9)...Cl(1)	0.860	2.385	3.144	147.70
Symmetry operation: (x, y, z); (-x,-y, -z)				